Ship Capsizing Analysis in Random Seas Using Non-standard Stochastic Averaging

L. Dostal*, E. Kreuzer* and N. Sri Namachchivaya **
*Institute of Mechanics and Ocean Engineering, Hamburg University of Technology, Hamburg, Germany
** Department of Aerospace Engineering, University of Illinois at Urbana-Champaign, Urbana-Champaign, USA

Summary. We study the dynamics of a ship in random seas as a perturbation of a Hamiltonian system. The random process across the energy levels of the Hamiltonian system is approximated by a Markov process, which is obtained by stochastic averaging. The noise due to wave excitation is a real stationary stochastic process. This is an extension to previous results where white noise excitation was used.

Introduction

The goal of the present research is to provide analytical relations for ship and sea state parameters which indicate the danger of large roll amplitudes or capsizing. Reduced order models are needed to perform an analytical analysis to this complicated problem. For modern ships like fast roll-on/roll-off ferries (roro ferries) and container vessels, the sudden appearance of roll motions due to waves from the front or rear in open seas leads to dangerous situations up to capsizing. On the other hand the current criteria of the International Maritime Organization (IMO) for the evaluation of the intact stability of ships [1] are based only on considerations of stability in still water and neither take into account the dynamic behavior of the vessel, nor the stochastic nature of the sea. Dangerous situations and accidents of ships at sea could often be avoided, if the risks could be predicted through improved and reliable calculation procedures. The difficulty in developing sufficient design rules lies in the very complex fluid-structure-interaction of the ship hull with the incident waves, as well as in the irregularity of the ocean waves. For a ship in unidirectional head or following waves no direct excitation of the roll motion can occur. But it is well known, that parametric resonance is possible due to oscillations of the roll restoring moment. A nonlinear model has to be used when analyzing large amplitude ship rolling. Theoretical and experimental studies of this issue were presented in [2]. Investigating ship motions in regular waves it is found, that parametric excited roll motions occur at a wave frequency, which is twice the roll motion eigenfrequency. Probabilistic modeling is necessary for a realistic description of ocean waves. In [3] the concept of the Grim effective wave [4] was extended to a traveling effective wave described by stochastic processes for its amplitude and phase. The governing equations for ship roll dynamics can be modeled by a softening spring type Duffing oscillator with additional cubic damping [5]. Analysis for the noisy Duffing-van der Pol oscillator was done in [6]. However, the case for the softening spring type Duffing oscillator was not analyzed. In the following we extend the results from [6] for ship roll motion under real noise excitation, which is crucial for the treatment of real problems in ship dynamics.

Description of Ocean Waves

The irregular long crested wave surface can be modeled by a superposition of infinitely many harmonic waves with wave numbers $k(\omega)$ and frequencies ω corresponding to a one-sided spectral density $S(\omega)$. To account for the irregularity of the wave surface, a random phase shift $\zeta(\omega)$ is added, which is uniformly distributed in the interval $[0, 2\pi)$. Such an irregular long crested wave surface can be written as

$$Z(x,t) = \int_0^\infty cos(\omega_e t - k(\omega)\xi + \zeta(\omega))\sqrt{2S(\omega)d\omega}. \tag{1}$$

Typical sea spectral densities are given in Fig. 4. We have to simplify the irregular wave surface $Z(x,t)$for further analysis, because there are infinitely many possibilities how waves can surround a ship. For most ship hulls a wave of the same length as the ship length will cause largest variations of righting lever. Therefore, $Z(x,t)$ is approximated by an effective wave (Fig. 1)

$$Z_{eff}(x,t) = \eta_c(t)\cos\left(\frac{2\pi}{L}x\right) + \eta_s(t)\sin\left(\frac{2\pi}{L}x\right) = \eta(t)cos\left(\frac{2\pi}{L}x + \psi(t)\right). \tag{2}$$

The wave length is chosen equal to the ship length L. The effective wave Z_{eff} consists of two harmonic components with random amplitudes $\eta_c(t)$ and $\eta_s(t)$ which can be transformed into a cosine wave with random amplitude $\eta(t)$ and random phase $\psi(t)$ by the well known transformation

$$\eta(t) = \sqrt{\eta_s(t)^2 + \eta_c(t)^2}, \qquad \psi(t) = \arctan\left(\frac{\eta_s(t)}{\eta_c(t)}\right), \tag{3}$$

or equivalently

$$\eta_s(t) = \eta(t)\sin(\psi(t)), \qquad \eta_c(t) = \eta(t)\cos(\psi(t)). \tag{4}$$

The random processes $\eta_c(t)$ and $\eta_s(t)$ are determined by solving the minimizing problem

$$minimize \quad I(\eta_s, \eta_c) = \int_{-L/2}^{L/2} \left(Z(x,t) - Z_{eff}(x,t)\right)^2 dx. \tag{5}$$

Solving for $\frac{\partial I(\eta_s,\eta_c)}{\partial \eta_s} = \frac{\partial I(\eta_s,\eta_c)}{\partial \eta_c} = 0$ gives

$$\eta_s(t) = \int_0^\infty f_s(k(\omega))sin(\omega_e t + \zeta(\omega))\sqrt{2S(\omega)d\omega}, \tag{6}$$

and

$$\eta_c(t) = \int_0^\infty f_c(k(\omega))cos(\omega_e t + \zeta(\omega))\sqrt{2S(\omega)d\omega}, \tag{7}$$

where the transfer functions are given by

$$f_s(k(\omega)) = \frac{2\pi \sin r}{\pi^2 - r^2}, \qquad f_c(k(\omega)) = \frac{2r \sin r}{\pi^2 - r^2}, \tag{8}$$

with $r = \frac{L}{2}k(\omega)$. The squared transfer functions f_c and f_s are shown in Fig. 2. By comparing the processes (6) and (7) with the irregular wave surface (1), we obtained the spectral densities S_{η_c} and S_{η_s} of the stochastic processes η_c and η_s, respectively, as

$$S_{\eta_s}(\omega) = 2S(\omega)f_s(k(\omega))^2, \qquad S_{\eta_c}(\omega) = 2S(\omega)f_c(k(\omega))^2. \tag{9}$$

The major advantage of the effective wave $Z_{eff}(x,t)$ in comparison with the irregular wave surface $Z(x,t)$ is, that we have a model for the excitation due to irregular seas depending only on two parameters η_c and η_s or η and ψ, respectively, which actually are stochastic processes with known spectral densities. If we set $\psi = 0$ or equivalently $\eta_s = 0$, we obtain the original Grim effective wave [4], i.e. the wave crest or trough is always amidships.

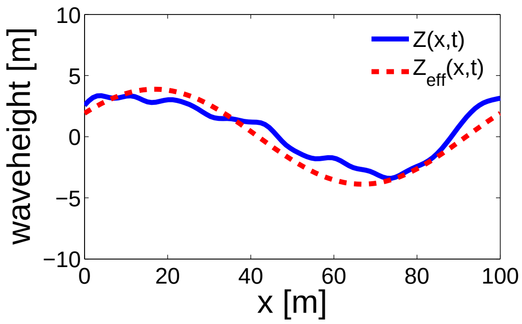

Figure 1: Irregular wave surface Z and effective wave approximation Z_{eff}

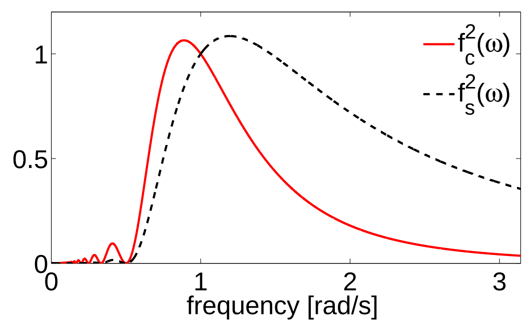

Figure 2: Squared transferfunctions

Roll Motion in Random Seas

The motion of the ship and the wave flow are described with respect to the coordinate system (x, y, z), where z is pointing upwards out of the fluid domain. The (x, y) plane defines the free water surface at rest, and the x axis coincides with the average forward direction of the ship. The center of gravity of the ship is located at the origin. It follows from linear ship motion analysis, that for symmetric floating bodies with respect to the x-z plane, the surge, heave, and pitch motions are decoupled from the sway, roll, and yaw motions. The forces $\mathbf{F}$ and moments $\mathbf{M}$ on the hull are determined by integrating the fluid pressure p over the wetted surface Ω of the ship hull

$$\mathbf{F} = -\iint_\Omega p\mathbf{n}d\Omega, \quad \mathbf{M} = -\iint_\Omega p(\mathbf{r} \times \mathbf{n})d\Omega. \tag{10}$$

Here, $\mathbf{n}$ is the unit normal vector on Ω and $\mathbf{r}$ is the corresponding position vector. The pressure distribution due to incident waves at a depth z below the calm water surface is

$$p = \rho g \zeta_a \frac{\cosh k(z+d)}{\cos kd}\cos(kx - \omega t) - \rho g z, \tag{11}$$

where d ist the water depth and ζ_a the wave amplitude. Higher order effects due to ship generated waves are neglected. The restoring forces of a ship in waves can be determined by the righting lever GZ. First the center of buoyancy Z has to be computed by integration of pressure over the wetted surface, which is obtained by computation of (10). The righting lever is the distance from Z to the center of gravity G. As can be seen in figure 3 we have a higher stability in wave trough and a lower stability in wave crest. Since the wave crest position and wave amplitude varies with time, we have also time varying restoring characteristics of the ship. We assume a quasi static behavior. This means that for the incident wave the ship is in static equilibrium with respect to heave and pitch. The righting lever function $GZ(\Phi, \eta, \psi) : \mathbb{R}^3 \to \mathbb{R}$ is computed for various roll angles Φ and for long crested waves of the same length as the ship length with an elevation of η. The wave crest is located at $\cos(2\pi x/L + \psi)$ in the ship coordinate system. The righting lever should be computed for all values which can be reached during computation, even if they are not relevant in praxis (e.g. very large roll angles). The rolling behavior of a ship can be represented by the following equation if heave and pitch motions are small

$$(I_{xx} + A_{xx}(\omega_n))\ddot{\Phi}(t) + b_1\dot{\Phi}(t) + b_3\dot{\Phi}(t)^3 + g \cdot \Delta GZ(\Phi(t), \eta(t), \psi(t)) = M(\eta(t), \psi(t)), \tag{12}$$

where I_{xx} is the roll moment of inertia, $A_{xx}(\omega_n)$ is the hydrodynamic added mass evaluated at the natural frequency ω_n, b_1, and b_3 are linear and cubic damping coefficients, g is acceleration due to gravity, Δ is the displacement. M is an additive excitation moment, which is small, if the ship travels in about the same direction as the waves. Here, the righting lever is a function of the roll angle ϕ, the wave phase ψ and the wave amplitude η. For further analytical analysis, $GZ(\Phi, \eta, \psi)$ is approximated by

$$GZ_{app}(\Phi, \eta, \psi) = q_1\Phi + q_2\Phi^3 + q_3\eta\cos(\psi)\Phi = q_1\Phi + q_2\Phi^3 + q_3\eta_c\Phi. \tag{13}$$

Here, we use cubic approximation in ϕ and harmonic approximation in ψ. For the following we define $\xi_t := \eta_c(t)$ and approximate M by

$$M(\eta(t), \psi(t)) = q_4\xi_t. \tag{14}$$

After some rescaling, equation (12) with GZ and M given by (13) and (14), respectively, can be written as

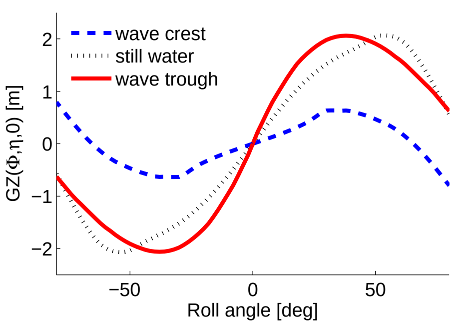

Figure 3: Righting levers for different waves amidships

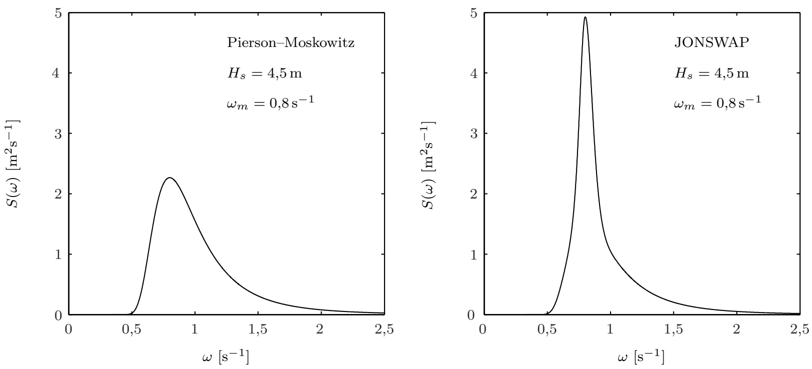

Figure 4: Pierson-Moskowitz spectrum and JONSWAP spectrum

$$\begin{aligned}\dot{x}(t) &= \frac{\partial H}{\partial y(t)},\\ \dot{y}(t) &= -\frac{\partial H}{\partial x(t)} - \varepsilon\frac{\partial H}{\partial y(t)}(\beta_1 + \beta_3 y(t)^2) + \sqrt{\varepsilon}(\nu_1 + x(t)\nu_2)\xi_t,\end{aligned} \tag{15}$$

with stationary wide band random process ξ_t and noise intensities $\nu_1,\ \nu_2$. Making use of the fact, that the hydrodynamic damping and excitation forces due to fluid-structure interaction are small, we can assume $\varepsilon << 1$ to be also a small scaling parameter. The Hamiltonian of (15) is

$$H(x, y) := \frac{y^2}{2} + \alpha_1\frac{x^2}{2} - \alpha_3\frac{x^4}{4}, \tag{16}$$

where $\alpha_1, \alpha_3 > 0$, and we use the abbreviation $Q(x, H) := 2H - \alpha_1 x^2 + \alpha_3\frac{x^4}{2}$.

Stochastic Averaging

The analysis for the Duffing oscillator with a two well potential was done in [6]. However, the case for the softening spring type Duffing oscillator was not analyzed. In the following we extend the results from [6] for equation (15) under non-white noise excitation. Equation (15) is the softening type Duffing oscillator with linear and cubic damping.
For practical problems it is crucial to consider real noise excitation. For the non-white noise case we need to determine the functions $x(t+\tau)$ and $y(t+\tau)$ in terms of $x(t)$ and $y(t)$. From (15) we get in the case $H < \alpha_1^2/(4\alpha_3)$ (non capsized case)

$$x(t) = b\ sn(qt; k), \qquad x(t+\tau) = b\ sn(qt + q\tau; k), \tag{17}$$

$$\begin{aligned}\frac{dx}{dt} &= y(t) = \sqrt{Q(x(t), H)} = bq\ cn(qt; k)dn(qt; k),\\ y(t+\tau) &= \sqrt{Q(x(t+\tau), H)} = bq\ cn(qt + q\tau; k)dn(qt + q\tau; k),\end{aligned} \tag{18}$$

where $q := a\sqrt{\frac{\alpha_3}{2}}$ and $k := \frac{b}{a}$, with $a := \sqrt{\frac{4H}{b^2\alpha_3}}$, $b := \sqrt{-\frac{-\alpha_1 + \sqrt{\alpha_1^2 - 4\alpha_3 H}}{\alpha_3}}$. From now on we omit the elliptic modulus k in the Jacobian elliptic functions sn, cn, dn and use the abbreviations $u := qt$, $sn := sn(u)$, $cn := cn(u)$, $dn := dn(u)$,

$sn_{t+\tau} := sn(u+q\tau)$, $cn_{t+\tau} := cn(u+q\tau)$, $dn_{t+\tau} := dn(u+q\tau)$. The time derivative of Hamiltonian for system (15) is given by

$$\frac{dH}{dt} = \varepsilon y^2(-\beta_1 - \beta_3 y^2) + \sqrt{\varepsilon} y(\nu_1 + x\nu_2)\xi_t. \tag{19}$$

Combining the first equation of (15) and (19), and using $y = \sqrt{2H - \alpha_1 x^2 + \alpha_3 \frac{x^4}{2}}$ obtained from (16), we get the system

$$\begin{aligned} \frac{dx}{dt} &= \sqrt{Q(x,H)}, \\ \frac{dH}{dt} &= \varepsilon Q(x,H)(-\beta_1 - \beta_3 Q(x,H)) + \sqrt{\varepsilon}\sqrt{Q(x,H)}(\nu_1 + x\nu_2)\xi_t. \end{aligned} \tag{20}$$

Applying Khashminskii's limit theorem ([7] on page 394) to system (20), we get an Itô stochastic differential equation for the energy level H. This motivates the following proposition.

Proposition 1. *The energy level H of the system* (20) *is determined by the Itô stochastic differential equation*

$$dH = m(H)dt + \sigma(H)dW, \tag{21}$$

where the drift $m(H)$ and diffusion $\sigma(H)$ are given by

$$\begin{aligned} m(H) =& \frac{1}{T(H)q(H)} \int_{-\infty}^{0} R_{\xi_t\xi_t}(\tau) \int_0^{4K(k)} \left(b(H)^2\nu_2^2 sn\ sn_{t+\tau} + \nu_1^2\right) \frac{cn_{t+\tau}dn_{t+\tau}}{cn_t dn_t} du\, d\tau + \\ &+ \frac{1}{T(H)} \int_0^{T(H)} Q(x(t),H)(-\beta_1 - \beta_3 Q(x(t),H))dt, \end{aligned} \tag{22}$$

$$\sigma^2(H) = \frac{4b(H)^2 q(H)}{T(H)} \int_{-\infty}^{\infty} R_{\xi_t\xi_t}(\tau) \int_0^{K(k)} cn\ dn\ cn_{t+\tau}\ dn_{t+\tau}(\nu_1^2 + b(H)^2\nu_2^2 sn sn_{t+\tau})\, du\, d\tau. \tag{23}$$

Here, $R_{\xi_t\xi_t}(\tau)$ is the autocorrelation of the excitation process ξ_t.

Proof. The system (20) has slow and fast oscillations, which are the energy and roll oscillations, respectively. Additionally the driving stochastic process ξ_t with spectral density S_{η_c} that fulfills sufficient mixing conditions. Therefore, we can apply Khashminskii's limit theorem [7]. In our case, the fast roll oscillation $x(t)$ is averaged by using the averaging operator $\mathbb{M}$ for periodic functions f, which is given by

$$\mathbb{M}(f(t)) := \frac{1}{T(H)} \int_0^{T(H)} f(t)dt, \text{ where } T(H) = \int_0^{T(H)} dt = 2\int_{-b(H)}^{b(H)} \frac{dx}{\sqrt{Q(x,H)}} = 4K(k).$$

The period $T(H)$ corresponds to a specific energy level H, and $K(k)$ is the elliptic integral of the first kind. Applying Khashminskii's limit theorem to system (20), and substituting (17), (18) and $dt = du/q$, we get for the diffusion $\sigma(H)$

$$\begin{aligned} \sigma^2(H) =& \mathbb{M}\left\{\int_{-\infty}^{\infty} R_{\xi_t\xi_t}(\tau)(\nu_1 + \nu_2 x(t))(\nu_1 + \nu_2 x(t+\tau))\sqrt{Q(x(t),H)}\sqrt{Q(x(t+\tau),H)}d\tau\right\} \\ =& \frac{b(H)^2 q(H)}{T(H)} \int_{-\infty}^{\infty} R_{\xi_t\xi_t}(\tau) \int_0^{4K(k)} cn\ dn\ cn_{t+\tau}\ dn_{t+\tau}(\nu_1^2 + b\nu_1\nu_2 sn + b\nu_1\nu_2 sn_{t+\tau} + b^2\nu_2^2 sn sn_{t+\tau})\, du\, d\tau. \end{aligned} \tag{24}$$

In analogy the drift $m(H)$ is given by

$$\begin{aligned} m(H) =& \mathbb{M}\left\{Q(x(t),H)(-\beta_1 - \beta_3 Q(x(t),H)) + \int_{-\infty}^{0} R_{\xi_t\xi_t}(\tau)(\nu_1 + x(t)\nu_2)(\nu_1 + \nu_2 x(t+\tau))\frac{\sqrt{Q(x(t+\tau),H)}}{\sqrt{Q(x(t),H)}}d\tau\right\} \\ =& \frac{1}{T(H)q(H)} \int_{-\infty}^{0} R_{\xi_t\xi_t}(\tau) \int_0^{4K(k)} \left(b^2\nu_2^2 sn\ sn_{t+\tau} + b\nu_1\nu_2 sn + b\nu_1\nu_2 sn_{t+\tau} + \nu_1^2\right) \frac{cn_{t+\tau}dn_{t+\tau}}{cn_t dn_t} du\, d\tau + \\ &+ \frac{1}{T(H)} \int_0^{T(H)} Q(x(t),H)(-\beta_1 - \beta_3 Q(x(t),H))dt. \end{aligned} \tag{25}$$

We get the expressions for $m(H)$ and $\sigma^2(H)$ as stated in Proposition 1 after canceling the terms which integrates to zero.

□

Remark 1. *The stochastic process H defined by the averaged equations* (21) *can be interpreted as the total energy variation of roll oscillation due to wave forces and hydrodynamic damping acting on the vessel. Each energy level H corresponds to specific oscillatory roll motion of the investigated vessel. The energy level H defines the roll angle and velocity by means of equation* (16)*. Therefore, the roll oscillations become larger with increasing energy Level H.*

The equations (22) and (23) contain Jacobian elliptic functions with time shift. This time shift can be eliminated by using the addition formulas of Jacobian elliptic functions. Therefore, the integral in (23) can be writen as

$$\begin{aligned}\int_0^{K(k)} cn\, dn\, cn_{t+\tau}\, dn_{t+\tau}(\nu_1^2 + b^2\nu_2^2 sn sn_{t+\tau})\, du\, d\tau =& \nu_1^2 cn_\tau dn_\tau\, I_1 + \nu_1^2 k^2 sn_\tau^2 cn_\tau dn_\tau (I_1 - I_2 - I_3)\\ &+ b^2\nu_2^2(I_4 + I_5 + I_6 + I_7),\end{aligned} \tag{26}$$

with

$$I_1 := \int_0^{K(k)} \frac{cn^2\, dn^2}{(1-k^2sn^2sn_\tau^2)^2}\, du,\ \ I_2 := \int_0^{K(k)} \frac{cn^4(1-k^2)}{(1-k^2sn^2sn_\tau^2)^2}\, du,\ \ I_3 := \int_0^{K(k)} \frac{k^2cn^6}{(1-k^2sn^2sn_\tau^2)^2}\, du,$$

$$I_4 := cn_\tau^2\, dn_\tau^2 \int_0^{K(k)} \frac{sn^2\, cn^2\, dn^2}{(1-k^2sn^2sn_\tau)^3} du,\ \ I_5 := k^2 sn_\tau^2\, cn_\tau^2\, dn_\tau^2 \int_0^{K(k)} \frac{sn^4\, cn^2\, dn^2}{(1-k^2sn^2sn_\tau)^3} du,$$

$$I_6 := -sn_\tau^2\, cn_\tau^2 \int_0^{K(k)} \frac{sn^2\, cn^4\, dn^2}{(1-k^2sn^2sn_\tau)^3} du,\ \ I_7 := -sn_\tau^2\, dn_\tau^2 \int_0^{K(k)} \frac{sn^2\, cn^2\, dn^4}{(1-k^2sn^2sn_\tau)^3} du.$$

The integrals $I_1, \ldots, I_6$ can all be solved in closed form in terms of complete elliptic integrals of the first, second, and third kind. The explicit evaluation of the drift and diffusin terms is presented in [8]. The integral in (22) can be computed in the same way in terms of complete elliptic integrals.

Stationary density

We now introduce the speed and scale measures, which transform the diffusion process (21) on its natural scale, where the drift is identically zero. This task is achieved via the transformation $S(x)$ given by

$$S(x) = \int^x s(x)dx, \ \ \text{where}\ \ s(y) = \exp\left(-2\int^y \frac{m(\theta)}{\sigma^2(\theta)} d\theta\right)$$

is called the scale density. After defining the speed density $\mu(y) = 1/(\sigma^2(y)s(y))$, the stationary density function p_{st} associated with (21) can be given in terms of

$$p_{st}(H) = \mu(H)[c_1 S(H) + c_2]. \tag{27}$$

The coefficients c_1 and c_2 are determined by the boundary and normality conditions. Following [10] the (left) boundaries can be classified as: Entrance, if $\Sigma_l(x_l) = \infty$ and $N_l(x_l) < \infty$; reflecting, if $\Sigma_l(x_l) < \infty$, $N_l(x_l) < \infty$, and $M(x_l) = 0$; exit, if $\Sigma_l(x_l) < \infty$. Here, $M(\cdot)$ is the speed measure, $\Sigma_l(x_l)$ is the time to reach the left boundary x_l starting in $x \in [x_l, x_r]$, whereas $N_l(x_l)$ is the time to reach $x \in [x_l, x_r]$ starting in x_l. These measures are given by

$$dM(y) = \mu(y)dy,\ \ \Sigma_l(x_l) = \int_{x_l}^x \left\{\int_\eta^x \mu(\xi)d\xi\right\} s(\eta)d\eta,\ \ \text{and}\ \ N_l(x_l) = \int_{x_l}^x \left\{\int_\eta^x s(\xi)d\xi\right\} \mu(\eta)d\eta. \tag{28}$$

If we assume a reflecting boundary at $H = \alpha_1^2/(4\alpha_3)$ (i.e. no capsizing), which is approximately the case for moderate noise intensities, then $c_1 = 0$. In this case a stationary solution of (29) exists and is given by

$$p_{st}(H) = \frac{c_2}{\sigma^2(H)} \exp\left(2\int_0^H \frac{m(H)}{\sigma^2(H)}\right). \tag{29}$$

Simulation

Data of a roro ferry [9] are used to compare the original system (15) with the averaged system (21). The process ξ_t is defined by the autocorrelation function

$$R_{\xi_t\xi_t}(\tau) = \frac{\sigma_z^2}{2\mu_1\mu_2(\mu_1^2-\mu_2^2)}(\mu_2\exp(\mu_1|\tau|) - \mu_1\exp(\mu_2|\tau|)), \qquad \text{where} \qquad \mu_{1,2} \ = -c\omega_n \pm \omega_n\sqrt{c^2-1}. \tag{30}$$

We use filtered white noise χ_1 to generate the random process $\xi_t =: \chi_1(t)$

$$d\chi_1(t) = (\chi_2(t) - a_1\chi_1(t))dt + b_1 dZ_t, \quad d\chi_2(t) = -a_2\chi_1(t)dt, \tag{31}$$

where $E[dZ_t] = 0$ and $E[dZ_t dZ_{t-\tau}] = \sigma_z^2\delta(\tau)$, where δ is the Dirac delta function. The simulation shows good agreement with the probability density function (29) of the systems (15) and (21), even in the region of large energy levels H. For combined additive and multiplicative as well as pure additive random excitation, this can be seen in Fig. 5 and Fig. 6, respectively. In the case of parametric resonance conditions, Fig. 6, there is a peak at about $H = 0.1$ which corresponds to large roll oscillations. Whereas in the case of additive excitation only, Fig. 5, there is no resonance phenomenon. Instead, there are random roll motions which return to the unforced steady state at $H = 0$.

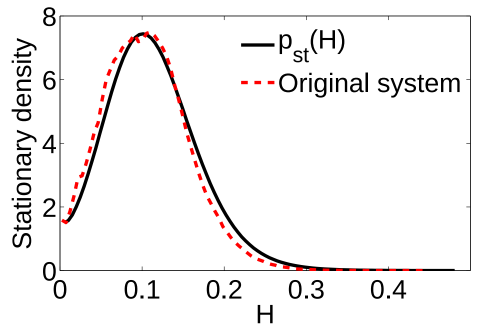

Figure 5: Comparison of simulation and stationary solution for $\alpha_1 = 1$, $\alpha_3 = 0.5$, $\beta_1 = 1$, $\beta_3 = 15$, $\nu_1 = 0.2$, $\nu_2 = 2$

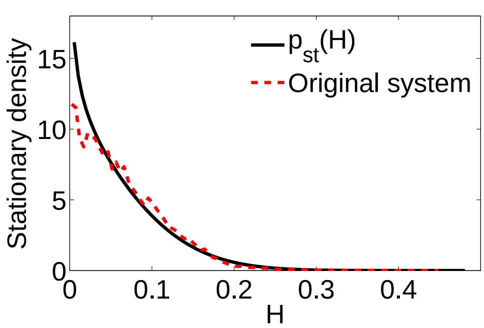

Figure 6: Comparison of simulation and stationary solution for $\alpha_1 = 1$, $\alpha_3 = 0.5$, $\beta_1 = 1$, $\beta_3 = 15$, $\nu_1 = 0.5$, $\nu_2 = 0$

Exit time

We are now looking for the mean time it takes for the roll motion to reach certain energy levels H_c starting at an initial energy level H. Therefore, we use the following result.

Theorem 1. (Namachchivaya [11]) *Let x_e be entrance boundary (i.e. $\Sigma_l(x_e) = \infty$ and $N_l(x_e) < \infty$) and let x_c be regular or exit boundary (i.e. $\Sigma_r(x_c) < \infty$), then the mean time to reach x_c starting at any $x \in [x_e, x_c]$ is given by*

$$u_e(x) = 2 \int_x^{x_c} \left[\int_z^{x_c} s(y)dy \right] \mu(z)dz. \tag{32}$$

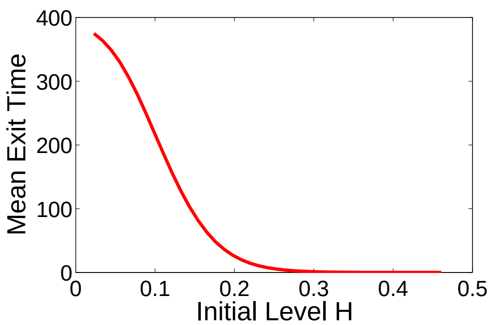

Figure 7: Exit time for $\alpha_1 = 1$, $\alpha_3 = 0.5$, $\beta_1 = 1$, $\beta_3 = 15$, $\nu_1 = 0.2$, $\nu_2 = 2$

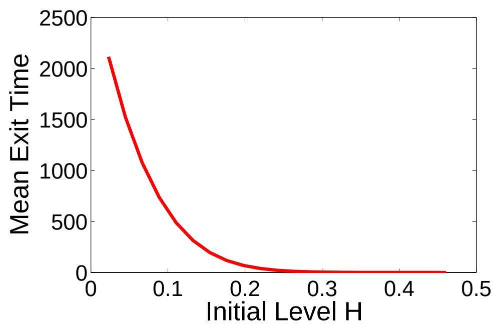

Figure 8: Exit time for $\alpha_1 = 1$, $\alpha_3 = 0.5$, $\beta_1 = 1$, $\beta_3 = 15$, $\nu_1 = 0.5$, $\nu_2 = 0$

In Fig. 7 the mean exit time (32) for capsizing is plotted in dependence on the initial energy level H for combined parametric and additive excitation. Here, the roll motion can reach the critical energy $H_c = 0.5$, where the ship can capsize within a few wave cycles. Therefore, parametric excited roll motion is a dangerous phenomenon, because the ship crew does not have enough time to avoid these dangerous conditions by maneuvering the vessel. The case of additive excitation, see Fig. 8, is less dangerous for the vessel, because large roll oscillation needs a longer time to develop.

Acknowledgement The authors are indebted to the DFG (Deutsche Forschungsgemeinschaft/German Research Foundation) for funding the project under contract Kr 752/29-1.

References

[1] IMO: *International code on intact stability, 2008.* London : International Maritime Organization, 2009 (res MSC.267(85))

[2] Oh, I. G. ; Nayfeh, A. H. ; Mook, D. T.: A theoretical and experimental investigation of indirectly excited roll motion in ships. In: *Phil Trans R Soc Lond A* 358 (2000), p. 1853 - 1881

[3] Bulian, G.: On an improved Grim effective wave. In: *Ocean Engineering* 35 (2008), no. 17 - 18, p. 1811 - 1825

[4] Grim, O.: Beitrag zu dem Problem der Sicherheit des Schiffes im Seegang. In: *Schiff und Hafen* 6 (1961), p. 490 - 497

[5] Arnold, L. ; Chueshov, I. ; Ochs, G.: Stability and capsizing of ships in random sea - a survey. In: *Nonlinear Dynamics* 36 (2004), p. 135 - 179

[6] Sri Namachchivaya, N. ; Sowers, R. B. ; Vedula, L.: Non-standard reduction of noisy Duffing-van der Pol equation. In: *Dynamical Systems* 16 (2001), no. 3, 223 - 245

[7] Khasminskii, R. Z.: A limit theorem for the solution of differential equations with random right-hand sides . In: *Theory Probab Appl* (1966), no.11, p. 390-405

[8] Dostal, L. ; Kreuzer, E.; Sri Namachchivaya, N.: Non-standard Stochastic Averaging of Large Amplitude Ship Rolling in Random Seas. *in preparation*

[9] Kreuzer, E. ; Sichermann, W.: Prediction of extreme ship motions in irregular waves. *5th EUROMECH Nonlinear Dynamics Conference.* Eindhoven (2005)

[10] Karlin, S. ; Taylor, M. H.: *A Second Course in Stochastic Processes.* New York : Academic Press, 1981

[11] Sri Namachchivaya, N. : Instability theorem based on the nature of the boundary behaviour for one dimensional diffusion. In: *Solid Mech Arch* 14 (1989), no. 3 - 4, p. 131 - 141